# The High-Resolution Streamer Chamber

This relatively new development offers high multitrack efficiency, nearly isotropic response, short memory time and electronic "triggerability."

Jack Sandweiss

As the contents of this issue of PHYSICS TODAY illustrate, the family of particle detectors that depend on electron multiplication processes in gases is a large and important one. Although the high-pressure streamer chamber is a relatively new development, it is a direct outgrowth of one of the branches of this family tree. (The reader interested in the "genealogy," as well as the physical and technical principles, will appreciate the excellent book by Peter Rice-Evans.[1])

The streamer chamber was invented in the early 1960's by G. E. Chikovani[2] and B. A. Dolgoshein.[3] The principle of operation is illustrated in figure 1. An intense electric field is applied to the gas volume of the chamber (within about 0.5 microsec) after the passage of a charged particle. Under the influence of the field, electrons left by the ionizing collisions of the particle are accelerated and form small "proto-sparks" or streamers, which delineate the trajectory of the particle. Normally, the chamber is photographed through the electrodes—which usually consist of wire grids or meshes—in what is known as the projection mode. Viewed this way, along the electric field, the streamers appear as small round dots along the track of the particle.

The development of streamer chambers for high-energy physics has, until our work at Yale, concentrated on the use of large volume chambers (about one cubic meter) operated at atmospheric pressure. Much of the current state of development in these chambers is due to the pioneering work at the Stanford Linear Accelerator Center.[4] Such chambers would typically operate with neon–helium mixtures (90%–10% or 70%–30%) electric fields of about 20 kV per cm and pulse durations of 10 to 20 nanosec. Streamer diameters are typically about 1 mm but, due to compromises in the optical system (to achieve adequate depth of focus), often have apparent diameters of several millimeters. A magnetic field of 10–15 kG is usually applied parallel to the electric field, for the measurement of charged-particle momenta. These chambers offer the advantage of high multitrack efficiency, nearly isotropic response, short (1 microsecond) memory time with the consequent capability of operating in $10^6$ particle-per-second beams and, finally, the important property of electronic "triggerability."

These atmospheric-pressure streamer chambers have been used in two general classes of experiments. With the addition of small internal hydrogen targets they have been used as "triggerable hydrogen bubble chambers"—but of course without the ability to see the vertex directly. The other general class includes a wide variety of experiments in which a triggerable isotropic track detector with high multitrack efficiency to allow visual pattern recognition is important. Typical spatial resolution for such chambers is about 300 microns. It is worth noting that so long as one is dealing with long-lived particles that can traverse the chamber, the precision of momentum determination depends quadratically on the chamber length and only linearly on the spatial resolutions. For this reason there has not been a strong motivation in the past to improve the spatial resolution of the chambers by methods that would result in smaller sizes.

After the discovery of the charmed particles,[5] there was a strong motivation to improve the spatial resolution of track detectors in general, and of the electron-

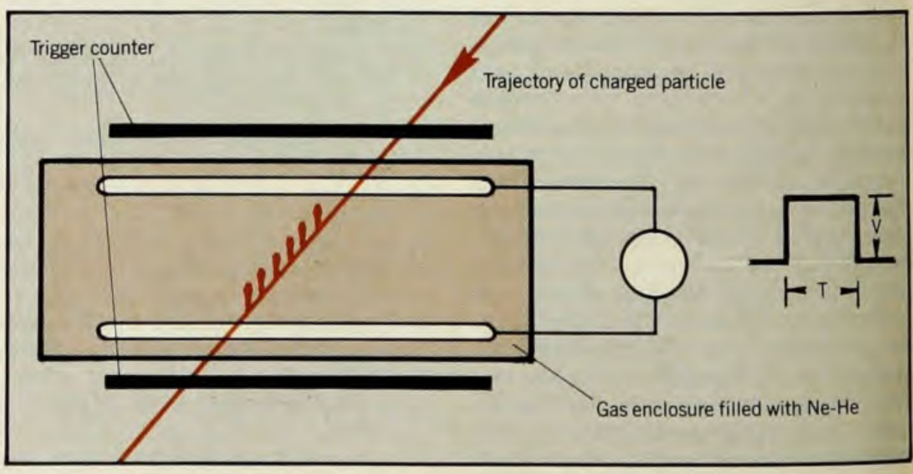


**Streamer-chamber operation** is illustrated in this schematic diagram. When the trigger counters register a charged-particle traversal, the pulser applies a high voltage $V$ for a time $T$ to the chamber electrodes. The electric field accelerates the electrons in the ionization trail of the particle, and a cascade avalanche and streamer develop from each primary ionization site. The pulse duration is short enough for the streamer pattern to delineate the particle path accurately. Figure 1

Jack Sandweiss is chairman of the physics department at Yale University.



0031-9228/78/3110-0040$0.50

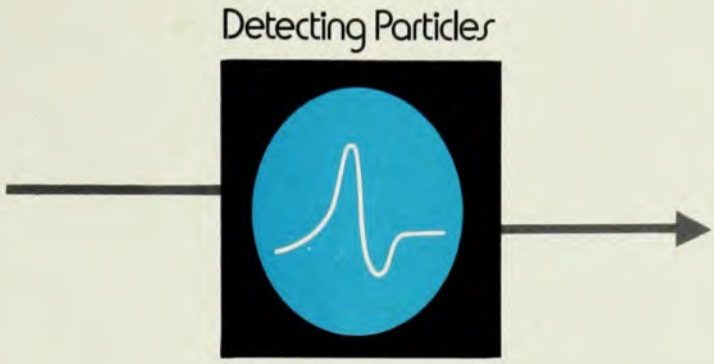


ically triggerable streamer chamber in particular, to the point where the tracks of the new particles could be observed and the production and decay vertices separately resolved. Such observations would allow direct measurements of charmed-particle lifetimes, would permit the search of those particles that would be missed by the usual techniques, which require detection of all the decay products, and would, in conjunction with other appartus, be extremely useful in charmed particle spectroscopy.

Charmed-particle lifetimes are estimated to be of the order of $10^{-13}$ sec.[5] Although there has as yet been no definitive experimental observation of a charmed-particle lifetime, it is interesting to note that one event that could be interpreted as a charmed-particle production (in a neutrino–nucleus collision) has been observed in an experiment that used nuclear emulsions and an electronic tagging system.[6] The decaying particle in this event traveled 182 microns, which corresponds to a flight time of $6 \times 10^{-13}$ sec or, with a reasonable interpretation of the event (accepting the charm hypothesis) to a proper time of approximately $2 \times 10^{-13}$ sec.

Charmed particles produced in high-energy hadron–hadron collisions can be expected to have laboratory velocities comparable to the velocity of the hadron–hadron center of mass. If a particle travels with a velocity equal to the center-of-mass velocity of a 300-GeV pion or proton striking a target nucleon at rest in the laboratory, it will travel in the laboratory with a time dilation factor $\gamma = 12.6$. A particle of proper lifetime $10^{-13}$ sec will thus travel 378 microns in the laboratory in one lifetime. This distance, taken together with typical decay angles, which can be estimated to be about 100 millirad, allow us to estimate the required resolution. It is straightforward to show that the standard deviation in the measurement of the distance between the production and decay points is, approximately, the point setting error (the spatial resolution) times the average decay angle. Thus spatial resolutions of 10–20 microns will give a resolution in decay distance corresponding to 0.26 to 0.53 of one lifetime at $10^{-13}$ sec and represent a reasonable target for the chamber resolution.

### The Yale streamer chamber

The principle we have used in designing the high-resolution chamber is a long-known scaling rule for avalanche formation in gases. Consider two ionization cascades as illustrated in figure 2. In case "$a$" the gas pressure is $p_0$, the applied electric field is $E_0$ and the duration of the applied field is $t_0$. In case "$b$" these values are scaled by a factor of 2. Since $E$ and $p$ are scaled by the same factor, the electron energies at the collision points are the same in both cases and because the density of $b$ is twice $a$ the mean free path in $b$ is half of its value in $a$. Since the electrons, on the average, will travel only half as far in $b$ as in $a$, but with the same distribution of energies, the avalanche $b$ will have half the physical dimensions of avalanche $a$ when both $a$ and $b$ have the *same total ionization*. Clearly $b$ will arrive at a given total ionization in half the time it would take $a$ to reach that ionization. This behavior can be generalized to an arbitrary scale factor $s$. Since the resolution in locating the position of the seed electron is inversely proportional to the diameter of the avalanche, we will want to make the scale factor as large as possible.

The foregoing is an oversimplified discussion of a complex phenomenon. For example, it neglects such effects as two-step ionizations, which could depend on various metastable atomic lifetimes so as to be important in a "fast" avalanche and not in a "slow" one. Most importantly, this picture neglects the space-charge effects that become important when the ionization level reaches a point where the space-charge fields are comparable to the applied electric field. At this state, as is well known, a streamer forms and begins to grow via different mechanisms—for example, photo-ionization. Nevertheless, the simple picture is a useful one, and experience has shown that it is a fairly

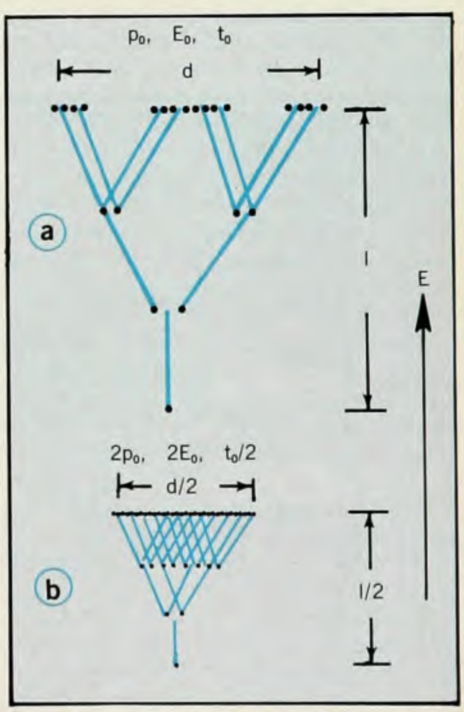


**Scaling principle in ionization avalanche formation.** In avalanche **a**, the gas pressure is $p_0$, the applied electric field is $E_0$, the duration of the field is $t_0$, and the physical dimensions of the avalanche are $d$ and $l$. In **b** these quantities are $2P_0$, $2E_0$, $t_0/2$, $d/2$ and $l/2$. Figure 2

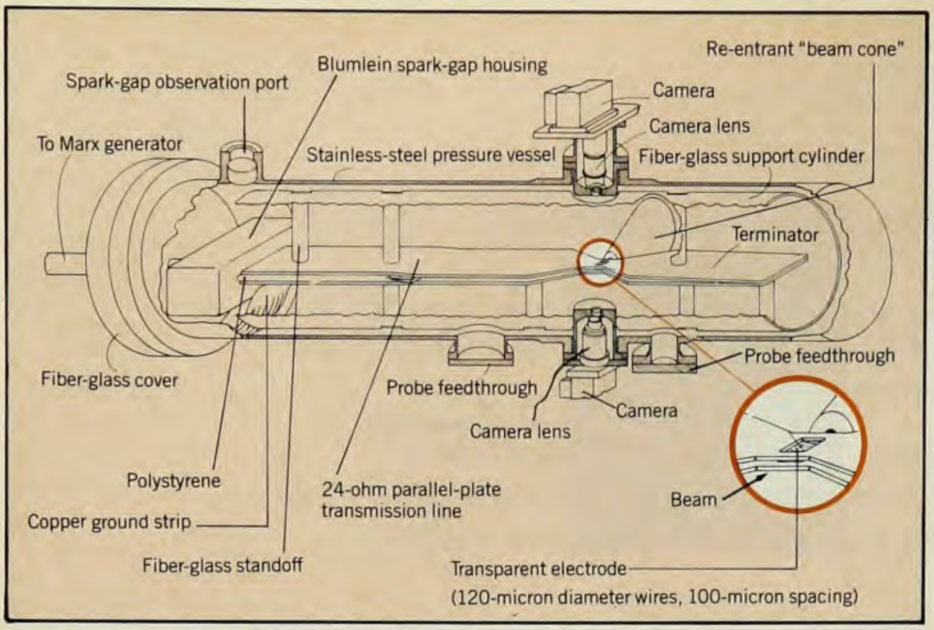


**High-resolution streamer chamber** developed at Yale University is seen in this cutaway sketch. The aim of the project was to scale the performance of atmospheric-pressure chamber by a factor of 20 in order to obtain a spatial resolution of 15 microns. Figure 3

accurate guide to expected performance.

About three years ago we began a program at Yale University,[7] with support from the Energy Research and Development Agency (now the Department of Energy) and also from the Fermi National Accelerator Laboratory, to develop a high-pressure streamer chamber that would provide spatial resolution in the 10–20 micron range. The basic parameter was the scaling factor, which was chosen to be between 20 and 40. More precisely the mechanical structures, such as pressure vessels, and the optical system were designed to operate up to 40 atmospheres. However, the pulsing system set the limit of operation to slightly more than 20 atmospheres. The table on page 44 below gives the basic parameters, with the scaling assumption, which are needed for 20-atm operation. The table also shows the values that have been achieved in our chamber system and, for reference purposes, the values for a typical atmospheric-pressure streamer chamber.

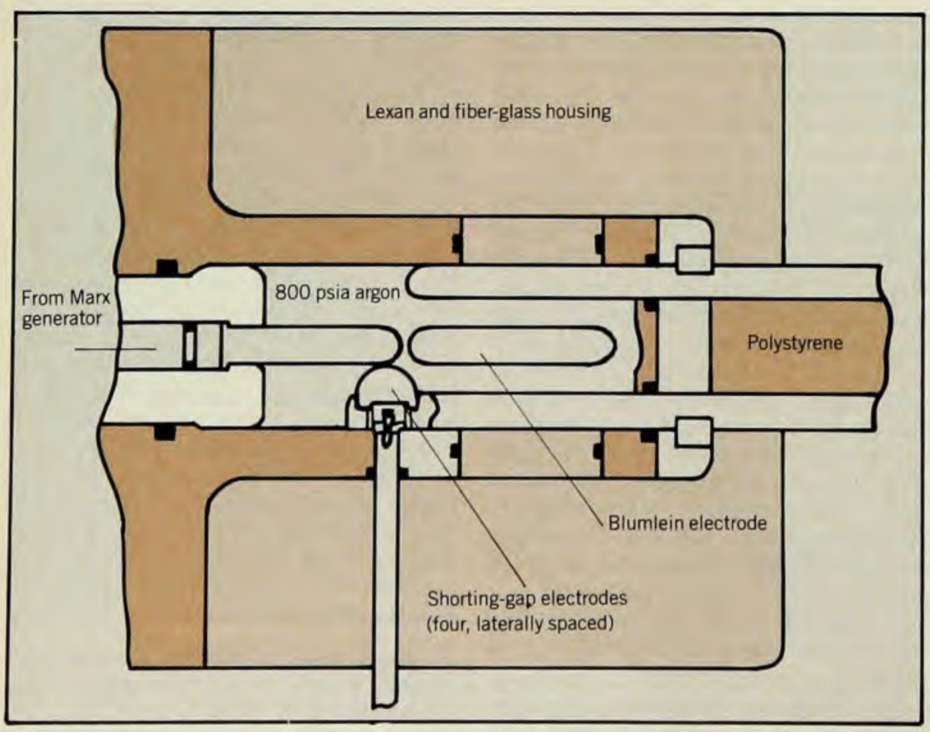


**Blumlein pulsing section for the Yale chamber.** The central electrode is charged from the Marx generator through a small gap, exaggerated in the sketch seen here. Figure 4

Figure 3 is a cutaway drawing of the Yale chamber. The electrodes of the chamber are an integral section of a parallel-plate transmission line which maintains a constant impedance of 24 ohms throughout its length despite changes in dimension and in dielectric filling. A parallel-plate Blumlein pulse-shaping section is built into one end of the line and this section is enclosed in a fiberglass and Lexan housing which holds, typically, 800 psia of argon. The line tapers in height (and width to maintain constant impedance) by means of transition sections that lead into and out of the chamber region. In this way the high electric field occurs only where it is needed, thus minimizing high-voltage breakdown problems. The pulse energy is absorbed in a terminator section that is, ideally, matched to the 24-ohm line over a bandwidth of about 1 GHz to avoid pulse reflections.

The entire assembly is supported in a fiberglass tube, which in turn rests in a stainless-steel pressure vessel containing the Ne–He gas. The use of the fiberglass support tube allows the entire line to be assembled outside the pressure vessel and then inserted as a unit. The chamber components that proved to be the least standard were the Blumlein pulser, the transparent electrodes and the terminator.

The construction of the Blumlein pulsing section is shown in figure 4. In ideal operation the Blumlein electrode would be charged to a voltage $V$, and when the output pulse is desired, it would be shorted to the lower electrode, instantaneously, all along its length perpendicular to the paper in figure 4. On the basis of known spark inductances and (10×) scale model tests, with avalanche transistors to model the spark gaps, we determined that four shorting gaps would suffice. The principal problem in such a design lies in achieving the precise synchronization required in firing the four gaps. Since the pulse width is 0.5 nsec, the gaps must fire in a time short compared to 0.5 nsec if the Blumlein system is to operate correctly. This was accomplished by charging the Blumlein electrode through a small spark gap. The charging gap produces ultraviolet light, which illuminates the shorting gaps and thus provides the initial electrons for the shorting gap discharges. Since the jitter in firing a spark gap is largely due to the "statistical wait" for the first electron, the jitter should be, and indeed is, very much reduced. A similar system is a coaxial Blumlein that had previously been shown by the University of Washington group[8] to produce fast rise-time pulses. The choice of argon gas for the Blumlein gaps is based on the high ultraviolet yield of argon discharges.

The principal problem with the Blumlein system was the electrical breakdown of the insulating support for the Blumlein

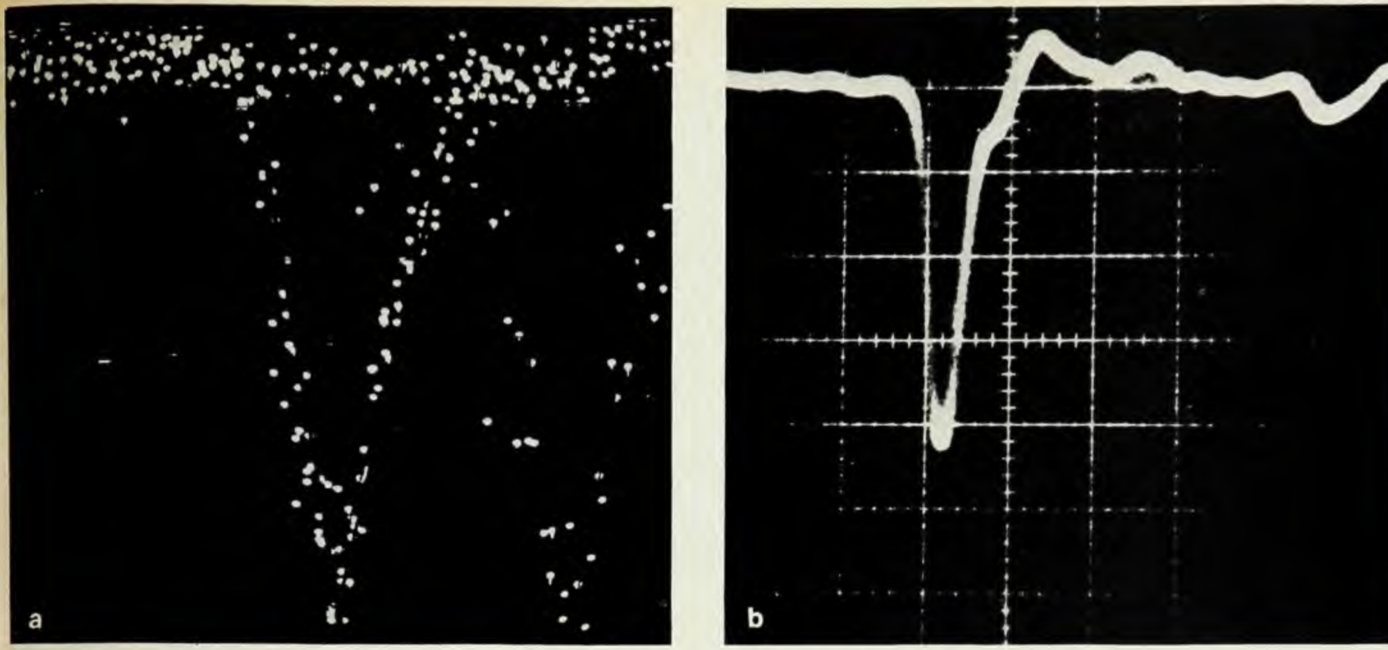


**Output pulse display.** The sampling oscilloscope display of a 90-kV pulse (a) has a rise time of about 70 picosec and shows a true picture of the waveform. Second peak in photo is the same signal, displaced by 1.3 nanosec for time base calibration. The real-time oscilloscope (b) has a rise time of about 0.8 nanosec, and is often used for convenience. Photo shows about fifty 150-kV pulses; sweep is 2 nsec/cm. Figure 5

electrode. In our earlier designs, the electrode was directly attached to the dielectric between the plates. The dielectric is required because of the Blumlein system requirement that the output line impedance be twice the impedance of the lines formed by the Blumlein electrode surfaces and the output electrodes. Because of the finite thickness of the Blumlein electrode, this condition could not be satisfied without dielectric loading of the output line. As shown in figure 3, the polystyrene dielectric ends in a transition section, which gradually changes the electrode spacing so as to keep the impedance constant. The solution to the problem lay in supporting the Blumlein electrode from its sides and accepting a slightly less than ideal geometry. This design has worked very well with no further high-voltage breakdown problems.

The output pulse is measured by capacitative dividers built into the ground electrode of the line. These are made of a 700-Å gold layer evaporated on a 0.001-inch Mylar spacer. Figure 5a shows a sampling oscilloscope record of the output pulse. The sampling system had a rise time of about 70 picosec and thus shows a true picture of the output waveform. The two peaks in figure 5a represent the same signal, displaced by 1.3 nsec for time-base calibration. The amplitude of the pulse in the figure is about 90 kV. The sampling oscilloscope system is rather delicate and noise-sensitive, requiring several hundred pulses to build up a useful picture. For convenience we often use a real-time oscilloscope that, as a system, has a rise time of about 0.8 nsec. Figure 5b shows such a real time picture of about 50 pulses. The amplitude of the pulses in figure 5b is 150 kV, and the sweep speed is 2 nsec per cm. The reflection at 9 nsec is due to the terminator, which is not perfectly matched.

The transparent electrodes of the chamber must carry the pulse current (of 6000 amperes or so), must have good geometry to establish the required uniform field in the chamber and must be adequately transparent. Our design utilizes 25-micron stainless-steel wires spaced every 100 microns. The major problem was the electrical connection of the wires to the 24-ohm line. We were unsuccessful in soldering the wires to their support frame, which is inserted into the line, and we also found that a variety of conducting epoxies failed under the high pulse current. The solution was an indium seal: The stainless-steel wires are wound over indium wires, which rest in triangular grooves in the back edges of the electrode support frame. After winding, and gluing the wires, the indium wires are pressed flat and indium flows around and between the electrode wires. The electrode assembly is then ready for insertion into the 24-ohm line.

The terminator must present a reflection-free load to the line and be capable of withstanding the high voltages and the pulse energy of roughly 0.5 joules. Our design is the parallel-plate analogue of a well known broadband coaxial terminator.[9] The terminator is, in essence, a resistive tapered line in which the resistance per unit length just compensates the decreasing surge impedance at any point in the taper. Not surprisingly, the total resistance, from the beginning of the terminator to the junction with the ground electrode, is just equal to the characteristic impedance of the line. The principal technical problem lay in producing the resistive electrode. The surface resistance of the electrode must be independent of frequency over the bandwidth required for the fast pulse. Because of the skin effect, the surface resistance will be independent of frequency only if the resistive layer is thin compared to the skin depth at the highest frequency (that is, the smallest skin depth) of interest.

Attempts to use thin metal films, about 2000 Å, were unsuccessful because of the vulnerability of the film to damage during repeated pulsing. The solution was to use "thick-film" resistors (0.001 inch) commercially manufactured to our specifications. Because of limitations on the maximum size of such resistors, the terminator was made of eight units. These resistors are of the same material as are used in hybrid circuit manufacture. This terminator design has been very satisfactory in all respects. In the interest of starting our tests within a reasonable amount of time, we used a terminator whose actual impedance value is slightly wrong for our line. This results in the reflection at 9 nsec (from the leading edge of the pulse), which can be seen in figure 5b.

The chamber is viewed with two lenses, which can image the chamber either at the film planes or at the photocathodes of the image intensifiers we now use (and shall discuss further on). The lenses are capable of resolving 80 line pairs per mm, and were originally designed and built for the Yale PEPR (Precision Encoding and Pattern Recognition) system by Perkin-Elmer Corporation to analyze bubble-chamber photographs. The two lenses have different focal lengths (4 inches and 6 inches) but are positioned so that they operate at the same magnification. The

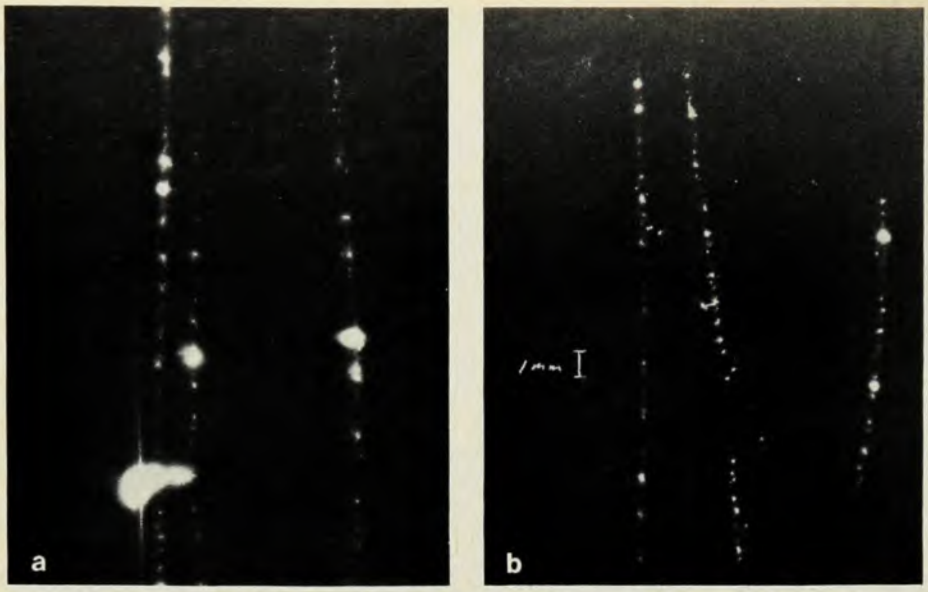

**$Ru^{106}$ decay electrons in the chamber.** At 150 psia of a Ne–He mixture, and no image intensification (**a**) several flares (bright areas) develop. Track length here is 4 cm. To reduce flaring, operation at lower total ionization per streamer was attempted (**b**). Here chamber pressure is 230 psia, and image intensification is 100. In both cases, pulses were 140 kV. Figure 6

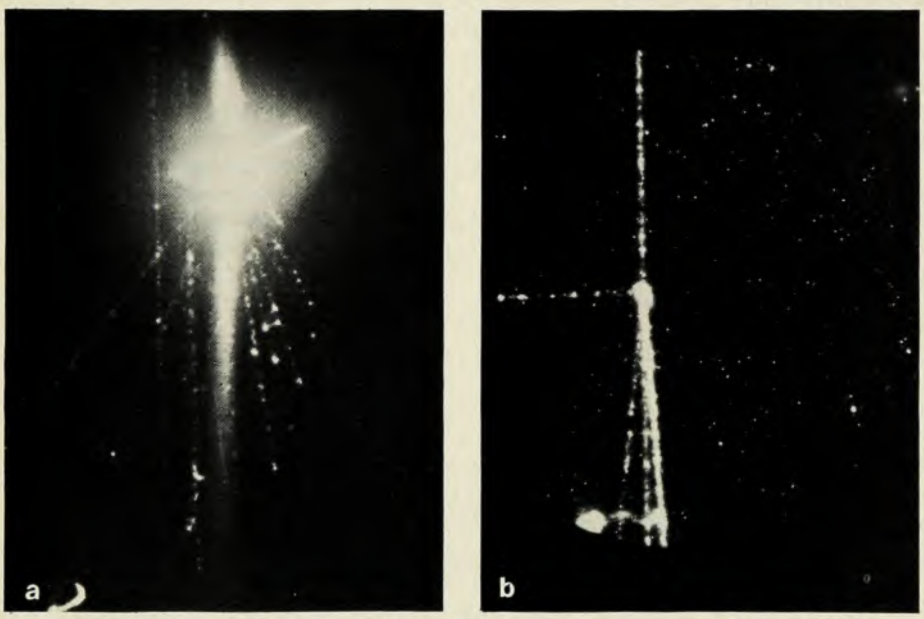

**Negative pion** interacting in chamber. Heavily ionizing nuclear fragments from this 200-GeV pion also cause flares (**a**). To cure this problem, microchannel image intensifiers were added to increase optical gain. Improved photo (**b**) was taken with 18-mm diameter microchannel intensifier, with gain of 10 000. Pressure was 370 psia. Figure 7

**Streamer-chamber parameters**

| | Std 1-atm chamber | Scaled to 20 atm | Yale chamber (24 atm) |
|---|---|---|---|
| Gas | spark-chamber neon (Ne/He = 90/10) | spark-chamber neon | |
| Electric field (kV/cm) | 10–20 | 200–400 | 333 |
| Pulse width (nsec, FWHM) | 10–20 | 0.5–1 | 0.5 |
| Pulse rise time (nsec) | 2–4 | 0.1–0.2 | 0.4 |
| Gap (cm) | ~30 | | 0.45 |
| Streamer diameter (mm) | ~1 | ~0.05 | ~0.05* |
| Circle of confusion of optical system (mm) | ~2–3 | | 0.05 |

* This is the apparent size of the streamer, due in part to the optical system. Furthermore, although the streamer diameter is 50 microns, the width of a track is 150 microns because the seed electron diffuses during the time delay between the passage of the particle and the application of the high-voltage pulse.

lenses typically operate at F/8 and produce a circle of confusion of 50 microns over a depth of field of 2 mm. The lenses, which are colinear, are displaced by 2 cm from the beam, giving 7-degree stereo.

### Testing the chamber

In the early tests of the chamber, with electrons from a $Ru^{106}$ source, the system was operated without image intensification. Kodak S.O. 143 film was used. Under these conditions visible tracks could be obtained at 150 psia (Ne–He) and pulse amplitudes of 140 kV. Figure 6a is a typical photograph under these conditions. Several important features are immediately evident. We see many small bright streamers consistent with our expected behavior. However, we also see large bright areas, which occur at a frequency of several per track. These are caused by streamers that have grown substantially larger than the normal ones. We believe these "flare" types originate from several seed electrons within one avalanche radius; that is, they are Landau fluctuations in the energy loss of the incident electrons.

Following this interpretation, we decided to operate at lower total ionization per streamer—at slower avalanche and streamer growth rates. This results in less light, so image intensification became necessary. We have used two types of image intensifier, both produced by the Electro-Optical Products Division of ITT. The first intensifier (model F4109) was a proximity-focussed diode with an optical gain of about 100 and a resolution of 50 line pairs per mm. With this tube it was possible to operate at Ne–He pressures of 230–250 psia. Figure 6b shows a typical picture, taken under these conditions, of $Ru^{106}$ decay electrons. We see that the problem of flares is gone. We also notice that the streamers are scattered about the "true" position of the track. This scatter is a result of diffusion of the seed electrons between the passage of the particle and the application of the high-voltage pulse, a time about 0.5 microsec. At this point the chamber was moved to Fermilab and set up in the M1 beam in the Meson Laboratory.

Although operation with an optical gain of 100 is excellent for minimum ionizing particles, it is not satisfactory for the observation of interactions within the chamber gas, which almost always produce heavily ionizing nuclear fragments. Figure 7a shows a photograph of a 200-GeV negative pion interacting in the chamber. The bright flare at the origin obscures the most interesting region for the study of short-lived particles. The "brush" of light extending downstream of the interaction vertex is due to light scattered into the camera from the electrode wires.

The cure for this flare problem, as for the previous one, lay in increased optical gain. We now operate the chamber with microchannel image intensifiers (Type F-4112 from Electro-Optical) with an optical gain of about 10 000 and a resolution of 26 line pairs per mm. Figure 7b shows a typical 200-GeV pion interaction in the chamber, operated with a microchannel plate intensifier at 370 psia Ne–He and 150-kV high-voltage pulse. The photo in figure 7b was taken with an 18-mm diameter tube, which was the only microchannel intensifier available on short notice for test purposes. We now use 25-mm tubes, which at our demagnification of 1.5 are adequate to view the 4-cm chamber length. With such large optical gain, the chamber is probably operating as an avalanche chamber rather than a streamer chamber. With the chamber operating in this mode, the tracks have an apparent width in space of 150–200 microns, and can be measured with a setting error of 15 microns.

We note that the effective chamber resolution is limited by the (thermal) diffusion of the seed electrons during the delay between the event and the high voltage pulse. Substantial research on various additives to reduce this diffusion has been carried out, but nothing useful has been found. The memory time of the chamber is easily controlled by the addition of sulfur hexafluoride just as is done in atmospheric chambers. We find that 20 psia partial pressure of dilute $SF_6$ (0.1 ppm $SF_6$ in Ne–He) produces a memory time of about one microsec.

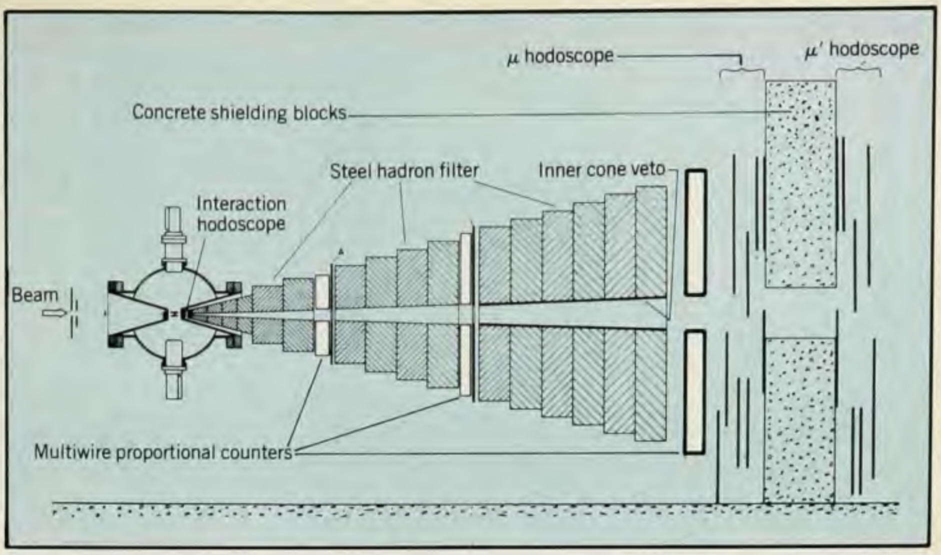


**Search for charmed particles.** Experimental set up seen here is used at the Fermi National Laboratory. Muons from the semileptonic decay of charmed particles penetrate the steel hadron filters. According to recent estimates of cross sections, the experiment should produce one charmed-particle event for every 100–200 photos of triggered interactions in the chamber. Figure 8

#### Utilization of the chamber

As an illustration of the use of a high-resolution streamer chamber we give a brief description of an experiment[7] currently underway at Fermilab to search for charmed particles. The experimental set up is illustrated in figure 8. Interactions of beam particles in the chamber signal themselves by providing two or more counts in the (scintillator) interaction hodoscope. Muons from the semi-leptonic decay of charmed particles penetrate the steel hadron filter and fire an appropriate series of counters in the A, B, $\mu$ and $\mu'$ hodoscopes. The chamber high voltage is triggered on the combination of a good beam track, an interaction and an apparent muon. Measurements have shown that ordinary hadronic events (no charm!) fool this trigger system about 0.1% of the time. Monte Carlo studies with various reasonable assumptions indicate that charmed events will trigger the system with an efficiency of 3% or so, so we expect an enhancement of a factor of 30 for charm production events in the pictures which will be taken. The chamber can operate with sufficient beam (about $10^6$ particles per second) to take one fiducial interaction picture every ten pulses. If recent indications of charmed-particle production cross sections (of approximately 10 microbarns for 400-GeV protons) are correct, the experiment should produce 100 examples or so after about one month of operation.

One can envision future developments in two main directions. The chamber itself can undergo continued modification and improvement, and the associated equipment can be very substantially improved over the example given above. The chamber could be used with a downstream spectrometer that measures charged-particle momentum and type, as well as the directions and energies of photons from neutral pion decay. Such a hybrid system would be a powerful instrument in studying the systematics of charmed-particle production and decay.

In forecasting the future evolution of the chamber itself, one direction is clearly feasible—that of increased size. Improvements in the high-voltage pulsing system would allow higher pressures, as would improved image intensifiers. Although modest gains (roughly 1.5 in voltage and 2 in optical gain) appear feasible, it is difficult at this time to foresee order-of-magnitude improvements in these systems. Nevertheless, chamber systems with several times the sensitivity and somewhat better resolution appear to be reasonable extrapolations of the technology described above. With such systems we can hope to obtain samples of about 1000 events of charmed-particle production in typical high-energy physics accelerator runs. A more speculative possibility is the use of short laser pulses, rather than high-voltage pulses, to develop the streamers. These laser pulses would offer large improvements in resolution and in data rate.

* * *

*The development of this chamber would not have been possible without the skill and dedication of many people. The author's colleagues on E-490 (see reference 7) have contributed enormously to all stages of the project. It is a special pleasure to acknowledge the patience, ingenuity and craftsmanship of Adrian Disco, Stanley Ladzinski and their associates at the Gibbs Laboratory instrumentation shop at Yale. Gary Cottingham of Brookhaven National Laboratory provided essential understanding and advice concerning the Blumlein system. We express our appreciation to John Cuny, Thomas Lynch and Harold Baker of the Electro-Optical Products Division of ITT for their generous and effective assistance to us in the use of their image intensifiers.*

#### References

1. P. Rice-Evans, *Spark, Streamer Proportional and Drift Chambers,* Richlieu, London (1974).
2. G. E. Chikovani, V. A. Mikhailov, V. N. Roinishvili, Phys. Lett. **6,** 254 (1963).
3. B. A. Dolgoshein, B. U. Rodionox, B. I. Luchkov, Nucl. Instrum. Meth. **29,** 270 (1964).
4. F. Bulos, A. Odian, F. Villa, D. Yount, "Streamer Chamber Development," SLAC Report No. 74 (1967).
5. T. Appelquist, R. M. Barnett, K. Lane, "Charm and Beyond," to be published in *Annual Review of Nuclear and Particle Physics,* **28** (1978).
6. A. L. Read *et al,* "Search for short-lived particles in high-energy neutrino interactions identified using a hybrid emulsion–spark chamber arrangement," Fermilab-Pub-78156-Exp 7551.247 (submitted to Physical Review).
7. M. Dine, D. Ljung, T. Ludlam. R. Majka, J. Marx, P. Nemethy, J. Sandweiss, A. Schiz, J. Slaughter, H. Taft, M. Atac, S. Ecklund, "Search for short-lived particles using a high-resoulution streamer chamber," Fermilab proposal No. 490.
8. R. Rohrbach, *Proceedings of the International Conference on Instrumentation for High-Energy Physics* (1973); page 161.
9. *Technique of Microwave Measurements,* (C. G. Montcomery, ed), MIT Radiation Laboratory Series, Boston Technical Lithographics, Inc (1963), page 725. □